Development and analysis of numerical models for the craniospinal system

Pierre Mollo

Laboratoire de Mathématiques de Reims UMR 9008

PhD. defense
February 3, 2023

ANR project: HANUMAN 18-CE45-0014-01

HANUMAN: Human and Animal NUmerical Models for the crANio-spinal system

- Numerical models of the craniospinal system for the **human** ...
- ... and the **marmoset**.
- Cerebral vascular structures evolution.
- Correlation of results between human and animal.

Figure: *Callithrix Jacchus*

My thesis :

- Study of the Blood - CerebroSpinal Fluid interaction (CSF).
- Study of the IntraCranial Pressure (ICP) autoregulation.
- Make real data and numerical models interact.

1. Biomedical context
2. Data processing
3. Fluid modelling
4. Model order reduction
5. State estimation
6. Results

Cerebrospinal system

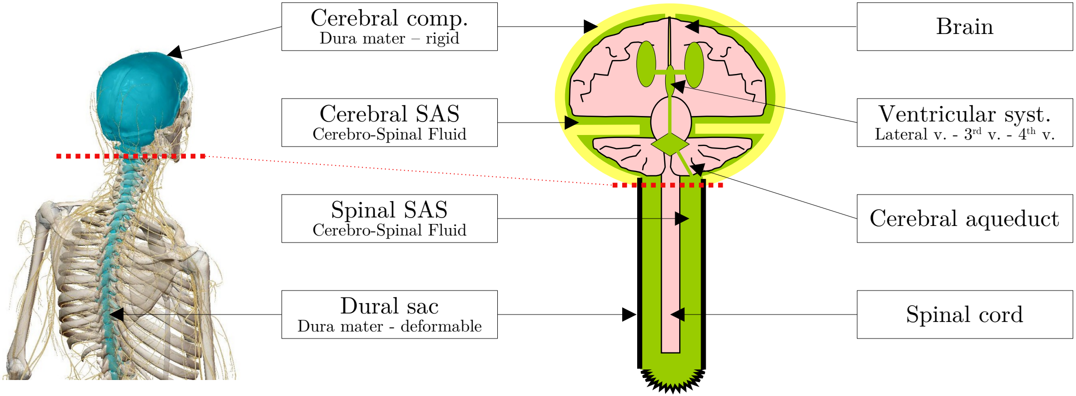

SAS: Sub-Arachnoid Space   CSF: CerebroSpinal Fluid

Cerebral compartment

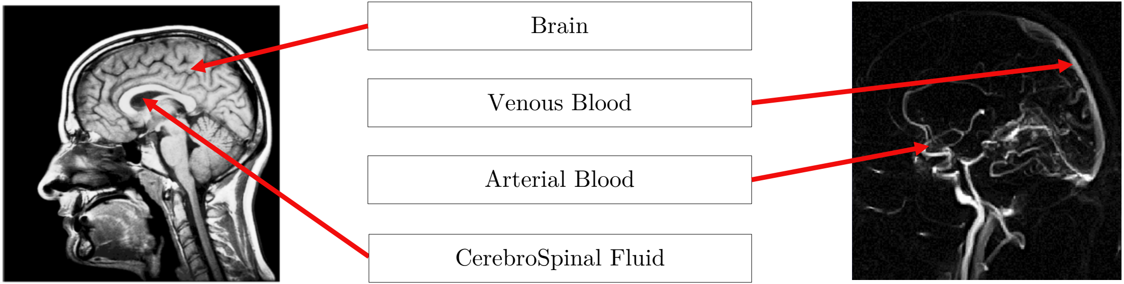

- Rigid compartment
- 4 incompressible volumes
- Dynamic system

- CerebroSpinal Fluid (CSF): $100 \sim 150[\mathrm{ml}]$
- Cerebral blood: 30% arterial (high pressure), 70% venous.

Cerebral compartment: **Volumes interactions**

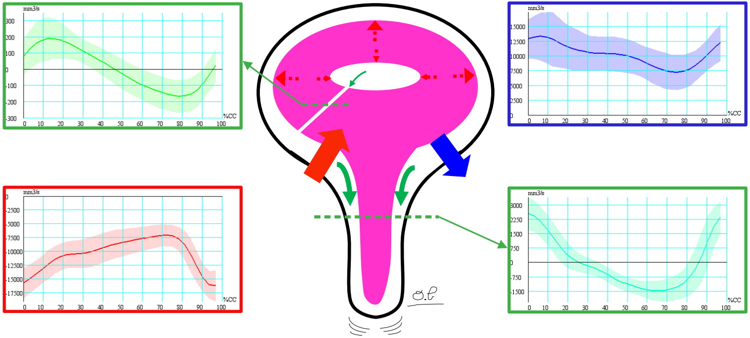

IntraCranial Pressure (ICP)

- ICP $=$ CSF pressure
- ICP $\simeq$ venous pressure
- ICP $\neq$ arterial pressure

ICP autoregulation

- ICP is crucial and must remain stable (Monro-Kellie)
- Rigid skull $\Rightarrow$ total volume is fixed
- Arterial peaks $\Rightarrow$ volumes displacements

Venous flow is dumped by CSF displacement

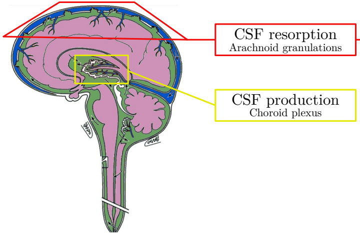

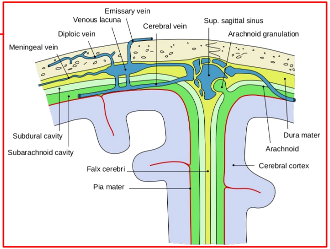

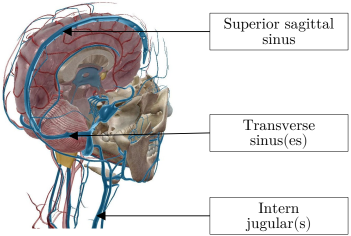

Classical CSF lifecycle

- Production by the choroid plexus, located in the ventricular system
- Resorption by arachnoid granulations mostly along sinuses

New point of view: **Glymphatic system**

Absorption and Resorption take place at the micro-circulation level continuously.

Non-optimal venous flow $\Rightarrow$ non-optimal CSF functioning

Cerebral compartment: **Vasculature**

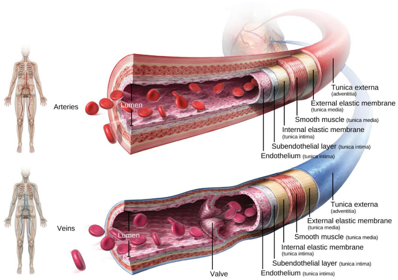

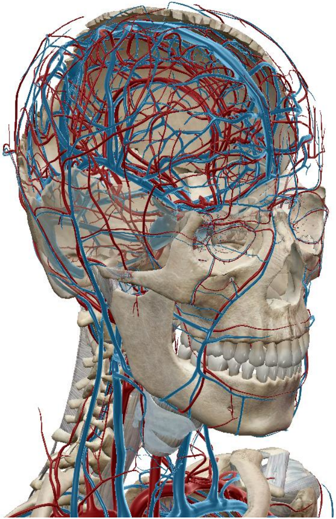

Veins

- Flexible ⇒ deformable
- non circular sections ⇒ collapsible
- Huge individual variability

Sinuses

- Sinus $\neq$ veins
- folds of dura mater
- Quasi-rigid
- ($\neq \sin(x)$)

- Flows up to down
- Focus on large scale vessels (>2mm $\oslash$)

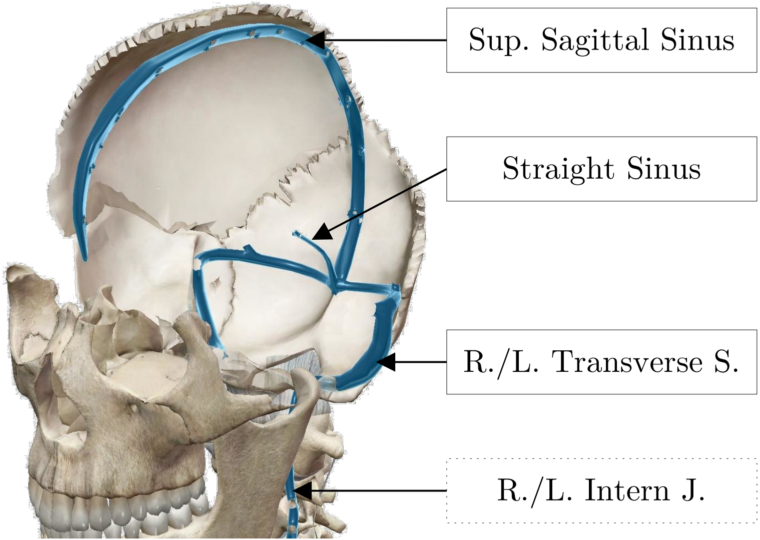

Cerebral compartment: **Blood Flow**

Blood

- Blood $\simeq$ plasma 54% and red cells 45%
- Red cells and other suspensions $\ll [\mathrm{mm}]$
- At macroscale $\rightarrow$ homogeneous, incompressible and Newtonian
- Slightly more viscous than water
- Circulation is periodic ($T \simeq 0.8$s)

Fluid model: Eulerian description

- $\mathbf{u}$ fluid velocity field
- p its pressure field
- Fluid dynamic $=$ incompressible Navier-Stokes equations

1 Biomedical context

2 Data processing

3 Fluid modelling

4 Model order reduction

5 State estimation

6 Results

Available data: **Morphology**

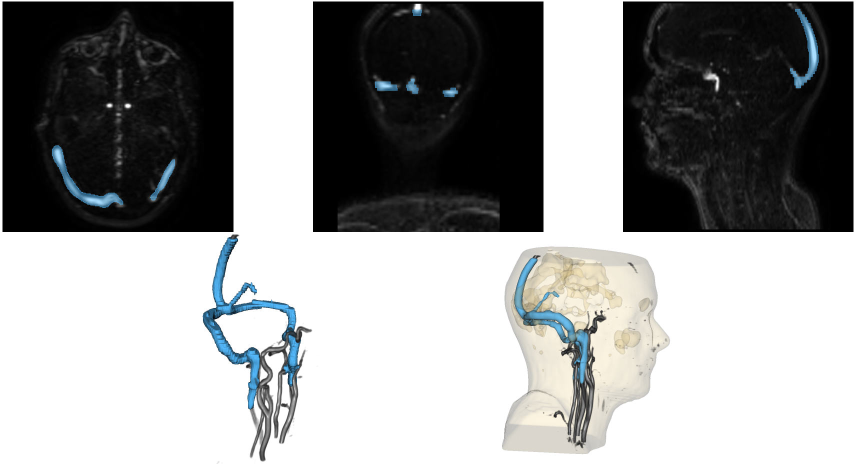

work Guillaume Dollé, software: *3D slicer* + in-house plugin.

Available data: **Morphology**

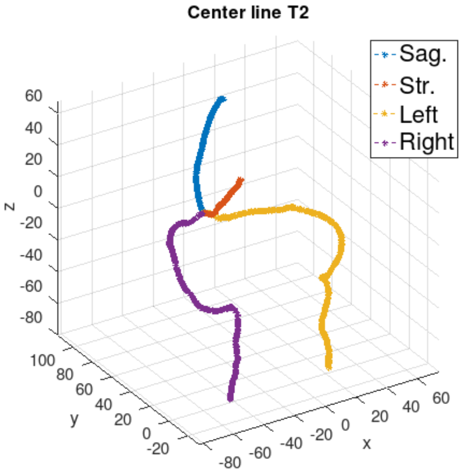

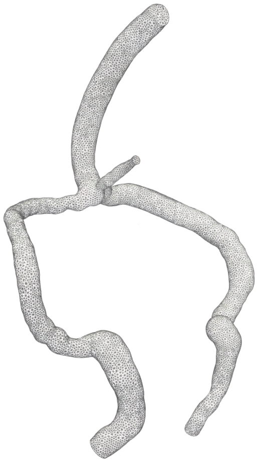

Mesh example for T2 individual from HyperPIC.

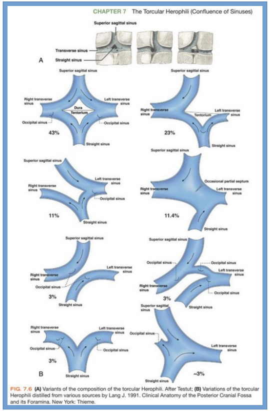

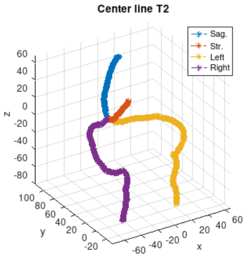

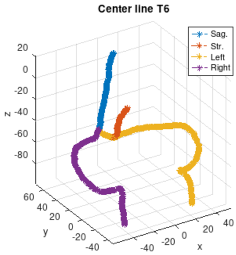

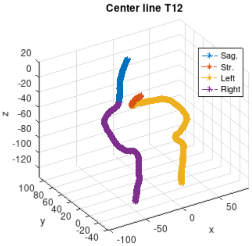

All healthy people

See [Streeter, 1915, M Das and Al Khalili, 2022], image from [Park et al., 2008].

Available data: **Velocity measurements**

Phase-Contrast MRI
(PC-MRI)

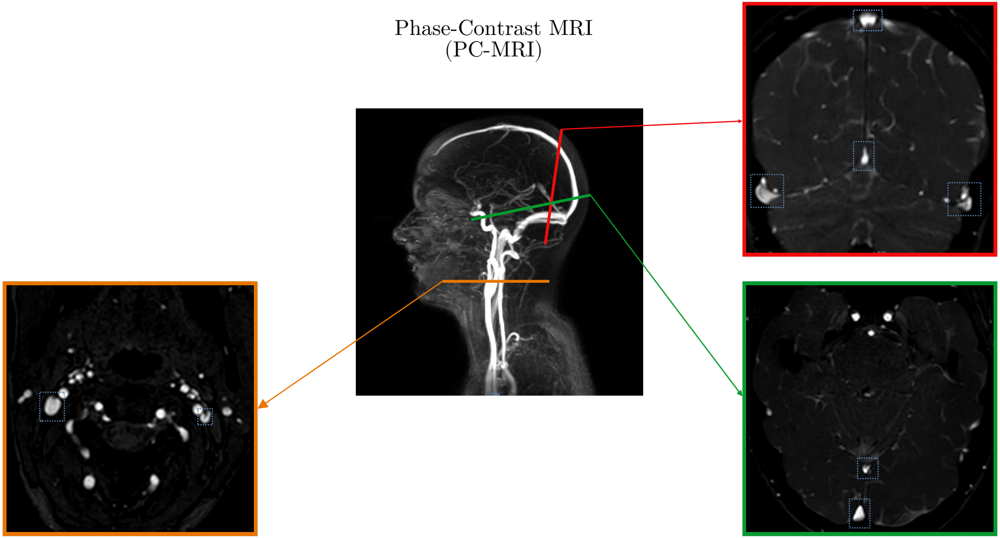

Available data: **Velocity measurements**

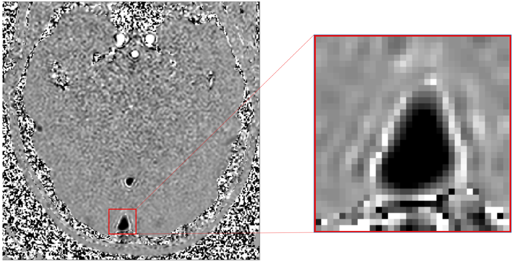

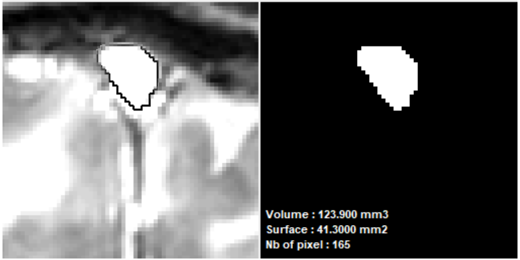

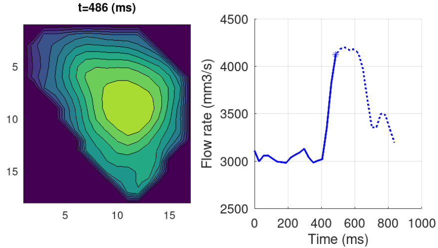

Velocity map

- velocity amplitude in the direction normal to the slice
- 1 measurement per (non-zero) pixel

Processed with the software *Flow* from CHIMERE team.

Available data: **Velocity measurements**

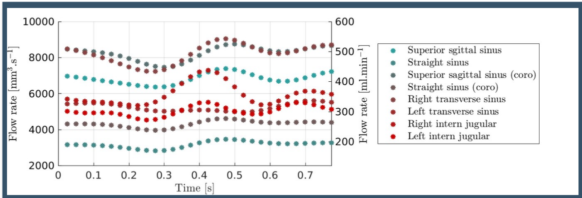

- Rescaling by group
- Master group = transverse sinuses

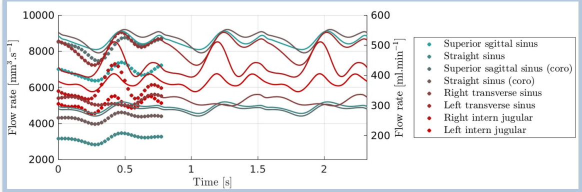

8 raw signals

- Interpolation by splines
- Displaced volumes are computed

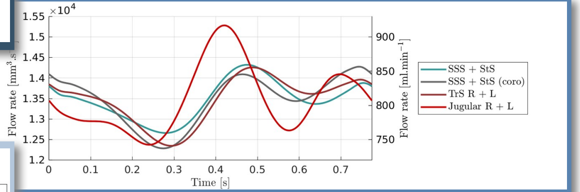

Use in numerical model

- Any time re-stepping possible
- Any number of cycles

https://gitlab.com/piemollo/phimod/frm

Available data: **Limitations and goals**

Limitations

- Only partial knowledge of the velocity field
- No pressure measurements (or invasive)
- High inter-individual variability and numerical approximation error
- Exact physiological parameters are unknown

Approach used

- Use numerical models to complete the information
- Link pressure and velocity with fluid model
- Develop semi-automatic and/or unified data processing
- Develop a data assimilation framework to manage the uncertainty

1 Biomedical context

2 Data processing

3 Fluid modelling

4 Model order reduction

5 State estimation

6 Results

Fluid modelling

Time discretization: $\delta t = T/K$, $t^k = k\delta t$, $0 \leq k \leq K$.
Velocity field: $\mathbf{u}^k = \mathbf{u}(t^k,.) \in V := \{v \in [H^1(\Omega)]^d,\ v_{|\Gamma_{\text{Wall}}} = 0, v_{|\Gamma_{\text{input}}} = \mathbf{g}\}$.
Pressure field: $p^k = p(t^k,.) \in Q := L^2(\Omega)$.

Navier-Stokes equations

$$\begin{cases} \rho\frac{\partial \mathbf{u}}{\partial t} + \rho(\mathbf{u}\cdot\nabla)\mathbf{u} - \eta\Delta\mathbf{u} + \nabla p = \mathbf{f} & \text{in } [0,T]\times\Omega \\ \nabla\cdot\mathbf{u} = 0 & \text{in } [0,T]\times\Omega \\ \mathbf{u} = \mathbf{0} & \text{on } [0,T]\times\Gamma_{\text{Wall}} \\ \mathbf{u} = \mathbf{g} & \text{on } [0,T]\times\Gamma_{\text{Input}} \\ \eta\frac{\partial \mathbf{u}}{\partial \mathbf{n}} + p\mathbf{n} = P\mathbf{n} & \text{on } [0,T]\times\Gamma_{\text{Output}} \\ \mathbf{u} = \mathbf{u}_0 & \text{on } \{0\}\times\Omega \end{cases}$$

- ρ fluid density
- η kinematic viscosity
- $\mathbf{f}$ external forces
- $\mathbf{g}$ inflow
- P external pressure
- $\mathbf{u}_0$ initial state

Remarks: no pressure issue with Neumann B.C. - solve using Taylor-Hood $\mathbb{P}^2 - \mathbb{P}^1$ FE - linearization using charac. method [Pironneau, 1982].

Fluid modelling: **Simulation framework**

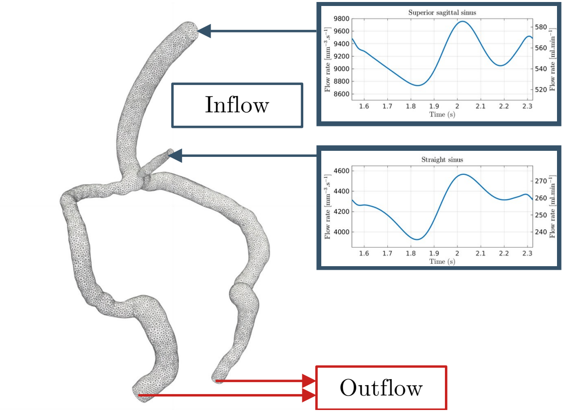

Simulation setup

- 3 cardiac cycles simulated
- 2 firsts are removed
- 800ts/cycle
- $\simeq$ 1.5M degrees of freedom
- 14h/simulation (4cores on ROMEO)
- Solver: FreeFem [Hecht, 2012]

Outflow

- Fully resistive Windkessel model
- Different resistances at each intern jugular

ROMEO: ROMEO Super Computer Center https://romeo.univ-reims.fr/

Fluid modelling: **Simulation results**

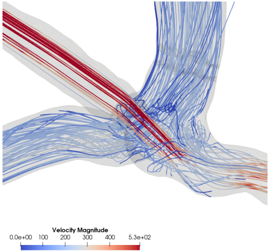

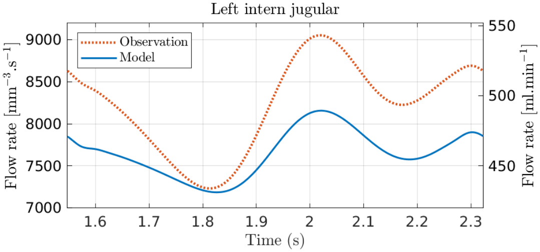

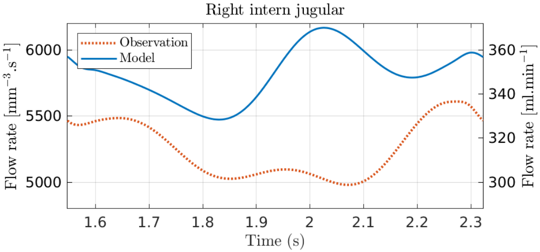

1 Biomedical context

2 Data processing

3 Fluid modelling

4 Model order reduction

5 State estimation

6 Results

Reduction: **Parameterized model**

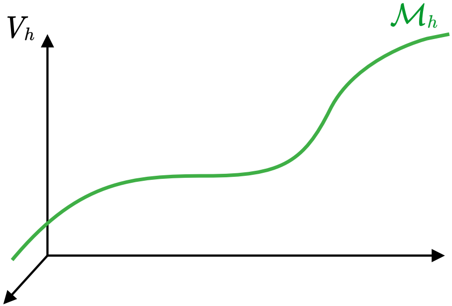

Parameterized model

Parameter:

$$\mu = (\eta, R1, R2) \in \mathcal{P}$$

Forward problem:

$$u : \ \mu \in \mathcal{P} \mapsto u(\mu) \in V_h^K$$

Manifold

$$\mathcal{M}_h = \{u^k(\mu) \in V_h, \ 1 \le k \le K, \ \mu \in \mathcal{P}\}$$

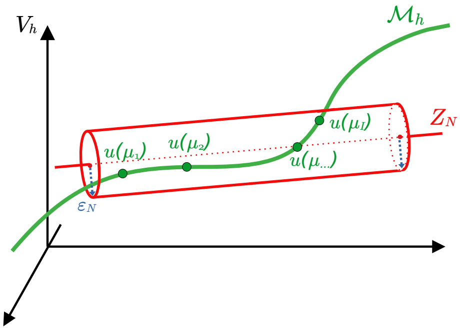

Generate the data base

- Forward problem solved using FE
- Snapshots computed with parameters:

$$S = \{u^1(\mu_1), \ldots, u^K(\mu_Q)\} \in V_h^{KQ}$$

Weak encapsulation

$$Z_N = \text{span}(\zeta_1, \ldots, \zeta_N)$$

$$\forall v \in S, \quad \|v - \pi_{Z_N} v\|_{V_h} \leq \varepsilon_N$$

Reduction: **Applications**

Online/Offline strategy

- **offline**: Reduced Basis building (on Supercomputers)
- **online**: use the RB
  - many query problem $\Rightarrow$ optimization, optimal control, uncertainty quantification, etc.
  - real time computation $\Rightarrow$ time dependent problems, digital twins
  - portable computation $\Rightarrow$ on micro-devices, smartphones or integrated in softwares

Several methods

- Greedy approach
- **Proper Orthogonal Decomposition** (POD)
- Empirical Interpolation Method (EIM) and variations

Reduction: **Applications**

Model compression

- *Parameter decomposition*
- *A priori* error estimate
- Greedy procedure
- Optimal nb. of *snapshots*

Galerkin solvers

- *Parameter estimation*
- Uncertainty quantification
- Optimal control
- Portable computation

- *Portable patient specific simulations*
- Chapters 4, 5 *(2019-2021)*

- *Inf-sup* stabilization
- Complex implementation

- *Exploit real MRI data*
- Chapters 4, 6-8 *(2021-2022)*

- State estimation framework built
- Many perspectives

Data compression

- *Snapshot* database
- **POD**, EIM

Projective solvers

- State estimation
- Data assimilation

Reduction: **Proper Orthogonal Decomposition**

Proper Orthogonal Decomposition [Quarteroni et al., 2016]

For $\mathbb{S} = \left[\underline{v}_1 | \dots | \underline{v}_{N_s}\right] \in \mathbb{R}^{\mathcal{N} \times N_s}$, build the correlation matrix $\mathbb{C} \in \mathbb{R}^{N_s \times N_s}$ given by:

$$(\mathbb{C})_{ij} = \left(v_i,\ v_j\right)_{V_h},\ 1 \leq i, j \leq N_s \quad \Leftrightarrow \quad \mathbb{C} = \mathbb{S}^t \mathbb{X} \mathbb{S}.$$

Given the Singular Value Decomposition, i.e. $\mathbb{C} = \mathbb{U}\Sigma\mathbb{V}^t$, and let $N \leq N_s$. We build $\mathbb{Z}_N \in \mathbb{R}^{\mathcal{N} \times N}$ such that

$$(\mathbb{Z}_N)_i = \frac{1}{\sqrt{\sigma_i}} \mathbb{S}(\mathbb{V})_i, \qquad i = 1, \dots, N.$$

Hence, we have the following result

$$\sum_{n=1}^{N_s} \|v_n - \pi_{Z_N} v_n\|_{V_h}^2 = \sum_{j=N+1}^{N_s} \sigma_j.$$

Reduction: **Proper Orthogonal Decomposition**

Proper Orthogonal Decomposition: Optimal Reduced Basis

Let $\mathcal{W} = \{\mathbb{W}_N \in \mathbb{R}^{\mathcal{N}\times N} | \mathbb{W}_N^t \mathbb{X} \mathbb{W}_N = \mathbb{I}_N\}$ and $W_N = \mathrm{span}(\mathbb{W}_N)$. The reduced basis built is optimal in the following sense:

$$\sum_{n=1}^{N_s} \|v_n - \pi_{Z_N} v_n\|_{V_h}^2 = \min_{\mathbb{W}_\mathrm{N} \in \mathcal{W}} \sum_{n=1}^{N_s} \|v_n - \pi_{W_N} v_n\|_{V_h}^2$$

Link with the Kolmogorov N-width

The decay of the correlation matrix spectrum, *i.e.* decay of $\sigma_1 \leq \cdots \leq \sigma_{N_s}$, reports on the Kolmogorov N-width and the problem compressibility:

- fast decay = small KNw = high compression
- slow decay = large KNw = low compression

Setup One time-snapshot

$Q = 1,\ K = 800 \Rightarrow 1$ simulation

Monolithic approach

- $v_i = (\mathbf{u}^i(\mu), p^i(\mu)) \in V_h \times Q_h = Z_h$
- $\langle (\mathbf{u}, p), (\mathbf{v}, q) \rangle_{Z_h} = \gamma \langle \mathbf{u}, \mathbf{v} \rangle_{V_h} + (1 - \gamma) \langle p, q \rangle_{Q_h}$
- *Hybrid* approach: $\gamma = \|\tilde{p}\| / \|\tilde{u}\|$

Relative mean quadratic Projection Error

$$\mathrm{RPE(S, Z_N)} = \sqrt{\frac{1}{N_s} \sum_{n=1}^{N_s} \frac{\| v_n - \pi_{Z_N} v_n \|^2_{V_h}}{\| v_n \|^2_{V_h}}}$$

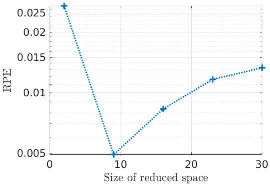

Velocity

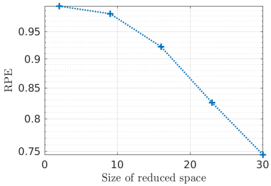

Pressure

Reduction: **Practical algorithm**

Standard POD

- $\mathbb{C}$ is a KQ-sized **full symmetric** matrix
- all the spectrum is needed
- only $N \ll QK$ eigen vectors are needed

…Full SVD is overkill.

Too expansive when $QK > 2000$.

Partial POD

- Spectrum estimation using QR-method iterations
- get only the N needed eigen vectors with power (or Lanczos) method

Allows to compute POD for large data set.

1 Biomedical context

2 Data processing

3 Fluid modelling

4 Model order reduction

5 State estimation

6 Results

Data fitting: **Measurement model**

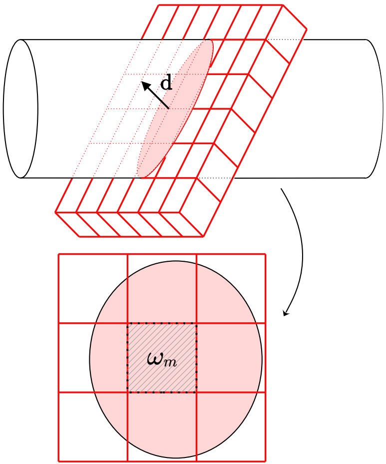

Similar to [Galarce et al., 2021b].

MRI measurement model

$$l_m(\mathbf{v}) = \int_{\omega_m} \mathbf{d} \cdot \mathbf{v} \, dx$$

- measures fluid velocity in the direction **d**
- voxel sizes depend on MRI resolution
- Nb of measure (possibly)

$$M = \text{nb slices} \times \text{nb pixels}$$

Observations are denoted

$$y^{\text{obs}} = L_M(\mathbf{v}) = \left(l_1(\mathbf{v}), \ldots, l_M(\mathbf{v})\right)^t \in \mathbb{R}^M.$$

Data fitting: **Minimization problem**

$$y^{\text{obs}} = L_M(u^{\text{true}})$$

We assume that the model is reasonable,

$$z^* = \arg \inf_{z \in Z_N} \|L_M(z) - y^{\text{obs}}\|^2_{\mathbb{R}^M,2}$$

Algebraic problem

$$\alpha^* = \arg \inf_{\alpha \in \mathbb{R}^N} \|\mathbb{L}_Z \alpha - y^{\text{obs}}\|^2_{\mathbb{R}^M}$$

- well posed if $M \leq N$
- can set linear constraints on α [Gong et al., 2019, Bui et al., 2022]

Decomposition in ROB

Using the ROB $Z_N = \text{span}(\zeta_1, \ldots, \zeta_N)$

$$z = \sum_{n=1}^{N} \alpha_n \zeta_n$$

Hence,

$$L_M(z) = \sum_{n=1}^{N} \alpha_n L_M(\zeta_n) = \underbrace{\mathbb{L}_M \mathbb{Z}_N}_{\mathbb{L}_Z \in \mathbb{R}^{M \times N}} \alpha$$

Data fitting: **Update space**

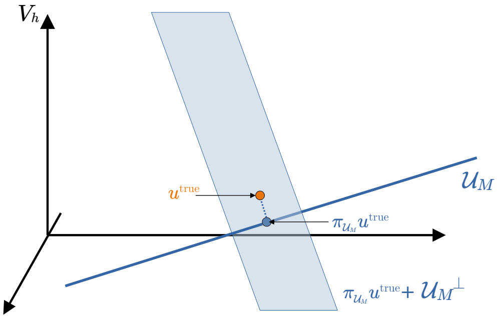

$$\mathcal{U}_M = \text{span}(w_1, \ldots, w_M)$$

where

$$l_m(v) = \langle w_m, v \rangle_{V_h}, \quad 1 \leq m \leq M$$

Data fitting: **Parametrized Background Data Weak approach**

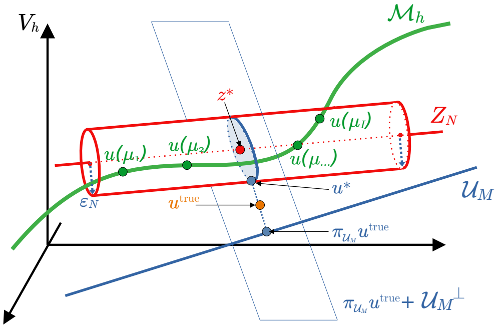

PBDW statement [Maday et al., 2015]

$$(z^*, v^*) = \arg \inf_{(z,v) \in Z_N \times \mathcal{U}_M} \|L_M(z+v) - y^{\text{obs}}\|^2_{\mathbb{R}^M} + \underbrace{\xi \|v\|^2_{V_h}}_{\text{regularization}}$$

$$L_M(v^*) = \underbrace{\sum_{m=1}^{M} \beta^*_m L_M(w_m)}_{\mathbb{L}_{\mathcal{U}} \in \mathbb{R}^{M \times M}}$$

$$(\alpha^*, \beta^*) = \arg \inf_{(\alpha,\beta) \in \mathbb{R}^N \times \mathbb{R}^M} \|\mathbb{L}_Z \alpha + \mathbb{L}_{\mathcal{U}} \beta - y^{\text{obs}}\|_{\mathbb{R}^M} + \ldots$$

1 Biomedical context

2 Data processing

3 Fluid modelling

4 Model order reduction

5 State estimation

6 Results

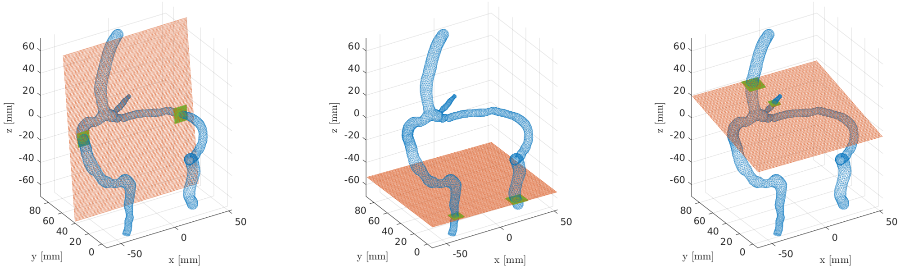

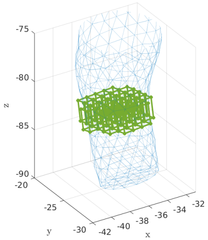

- $M = 263$ measurements
- Measurements are possibly correlated
- Synthetic measurements based on real MRI protocol

Training set (reduced basis)

$Q = 8,\ K = 800 \Rightarrow 6400$ snapshots

Test set

$Q = 2,\ K = 800 \Rightarrow 1600$ snapshots
(not in the training set)

Relative mean quadratic Estimation Error

$$\mathrm{REE}(\mathrm{Z_N}, \mathrm{L_M}) = \sqrt{\frac{1}{\#\mathcal{S}^{\text{test}}} \sum_{v \in \mathcal{S}^{\text{test}}} \frac{\|v - v^*\|_{\cdot}^2}{\|v\|_{\cdot}^2}}$$

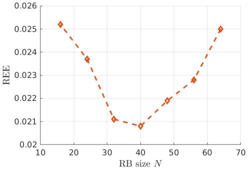

Velocity

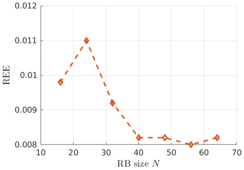

Pressure

Results: **Real data**

- Simulation and reduction frameworks ready
- State estimation framework ready
- Synthetic measurements are based on real MRI protocol

- Mesh geometry not precise enough
- Voxel location not precise enough

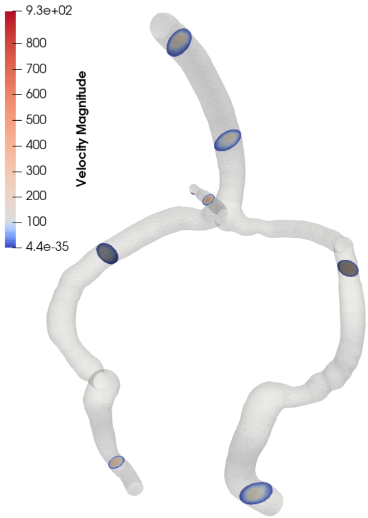

Conclusion and Perspectives

Conclusion

- Frameworks are built
- Pipeline from raw data to realistic simulations is built
- Encouraging results with synthetic data
- Real data are ready to be integrated

Perspectives

- Improve the geometry and fluid model
- Improve the estimation method
  (*e.g.* non-linear approaches, physics-based constraints)
- Improve the monolithic reduction

Some images in this document are used by courtesy of Visible Body and O. Balédent.

References

Bui, D.-Q., Mollo, P., Nobile, F., and Taddei, T. (2022).
A Component-Based Data Assimilation Strategy with Applications to Vascular Flows.

Galarce, F. (2021).
Inverse problems in hemodynamics. Fast estimation of blood flows from medical data.
phdthesis, Inria Paris ; Sorbonne Universite ; Laboratoire Jacques-Louis Lions.

Galarce, F., Lombardi, D., and Mula, O. (2021a).
Reconstructing haemodynamics quantities of interest from Doppler ultrasound imaging.
International journal for numerical methods in biomedical engineering, 37(2):e3416.
Place: England Publisher: Wiley.

Galarce, F., Lombardi, D., and Mula, O. (2021b).
State Estimation with Model Reduction and Shape Variability. Application to biomedical problems.
arXiv:2106.09421 [cs, math].
arXiv: 2106.09421.

Girault, V. and Raviart, P.-A. (1986).
Finite Element Methods for Navier-Stokes Equations, volume 5 of *Springer Series in Computational Mathematics*.
Springer Berlin Heidelberg, Berlin, Heidelberg.

Gong, H., Maday, Y., Mula, O., and Taddei, T. (2019).
PBDW method for state estimation: error analysis for noisy data and nonlinear formulation.
arXiv:1906.00810 [math].
arXiv: 1906.00810.

Hecht, F. (2012).
New development in FreeFem++.
Journal of Numerical Mathematics, 20(3-4):251–265.

Hesthaven, J. S., Rozza, G., and Stamm, B. (2016).
Certified Reduced Basis Methods for Parametrized Partial Differential Equations.
SpringerBriefs in Mathematics. Springer International Publishing, Cham.

M Das, J. and Al Khalili, Y. (2022).
Jugular Foramen Syndrome.
In *StatPearls*. StatPearls Publishing, Treasure Island (FL).

Maday, Y., Patera, A. T., Penn, J. D., and Yano, M. (2015).

A parameterized-background data-weak approach to variational data assimilation: formulation, analysis, and application to acoustics.
International Journal for Numerical Methods in Engineering, 102(5):933–965. _eprint: https://onlinelibrary.wiley.com/doi/pdf/10.1002/nme.4747.

Park, H. K., Bae, H. G., Choi, S. K., Chang, J. C., Cho, S. J., Byun, B. J., and Sim, K. B. (2008).
Morphological study of sinus flow in the confluence of sinuses.
Clinical Anatomy, 21(4):294–300. _eprint: https://onlinelibrary.wiley.com/doi/pdf/10.1002/ca.20620.

Pironneau, O. (1982).
On the transport-diffusion algorithm and its applications to the Navier-Stokes equations.
Numerische Mathematik, 38(3):309–332.

Quarteroni, A., Manzoni, A., and Negri, F. (2016).
Reduced Basis Methods for Partial Differential Equations, volume 92 of *UNITEXT*.
Springer International Publishing, Cham.

Streeter, G. L. (1915).
The development of the venous sinuses of the dura mater in the human embryo.
American Journal of Anatomy, 18(2):145–178. _eprint: https://onlinelibrary.wiley.com/doi/pdf/10.1

Taddei, T. (2017).
An Adaptive Parametrized-Background Data-Weak approach to variational data assimilation.
ESAIM: Mathematical Modelling and Numerical Analysis, 51(5):1827–1858.
Number: 5 Publisher: EDP Sciences.

Verfürth, R. (1984).
Error estimates for a mixed finite element approximation of the Stokes equations.
RAIRO. Analyse numérique, 18(2):175–182.
Number: 2 Publisher: EDP Sciences.

State estimation with noise

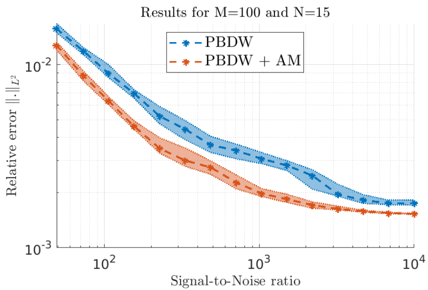

- Gaussian noise
- Dense random measurements
- AM: Artificial Measurements (based on weak free-divergence)

[Taddei, 2017, Gong et al., 2019, Bui et al., 2022]

Taylor-Hood FE convergence w.r.t. space step

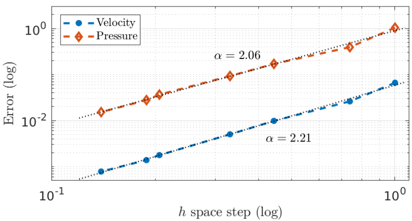

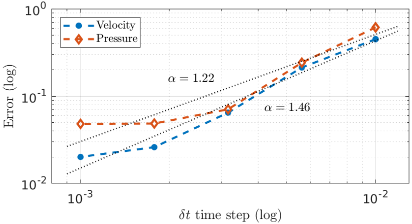

Field	Space convergence	Time convergence
Velocity $\|\|.\|\|_{L^2}$	3	1
Velocity $\|\|.\|\|_{H^1}$	2	1
Pressure $\|\|.\|\|_{L^2}$	2	1

[Girault and Raviart, 1986, Verfürth, 1984]